Primary frequency regulation supported by battery storage systems in power systems dominated by renewable energy sources

Turk, Ana; Sandelic, Monika; Noto, Giancarlo; Pillai, Jayakrishnan Radhakrishna; Chaudhary, Sanjay K.

Published in:
The Journal of Engineering

DOI (link to publication from Publisher):
10.1049/joe.2018.9349

Publication date:
2019

Document Version
Publisher's PDF, also known as Version of record

The Journal of Engineering

The 7th International Conference on Renewable Power Generation (RPG 2018)

IET Journals
The Institution of Engineering and Technology

Primary frequency regulation supported by battery storage systems in power system dominated by renewable energy sources

eISSN 2051-3305
Received on 5th November 2018
Accepted on 10th January 2019
E-First on 28th June 2019
doi: 10.1049/joe.2018.9349
www.ietdl.org

Ana Turk[1] ✉, Monika Sandelic[1], Giancarlo Noto[1], Jayakrishnan R. Pillai[1], Sanjay K. Chaudhary[1]

[1]*Department of Energy Technology, Aalborg University, Aalborg, Denmark*

✉ *E-mail: ana.turkica@gmail.com*

Abstract: In recent years, the transition process towards clean energy has caused many challenges to power systems, especially in the field of operation and power system control. Conventional generators, which have been providing ancillary services to maintain stability and reliability to the system, are being replaced by intermittent renewable generators. Therefore, maintaining system quality and stability in terms of power system frequency control is one of the major challenges that require new resources and system integration. Battery energy storage systems (BESSs), as fast-acting energy storage systems, with the capability to act as a controllable source and sink of electricity are one of the prominent solutions for system services. This study investigates the primary frequency control provision from BESSs to the renewable energy sources dominated power system. The simulation results for various cases have shown that integration of BESSs has significantly improved power system frequency stability.

1 Introduction

Denmark is an example of a coherent integrated system, which includes all energy sectors and has a high amount of renewable energy sources (RES) [1]. In 2016, the share of wind power production corresponded to 42% of the total Danish electricity consumption. One of the primary challenges, concerning wind power generation in the future, is to meet 50% of electricity consumption in 2020 [2]. It is expected that the share of RES in electricity production will be increased to 90% by 2025 [3]. Therefore, changes in electricity production have brought new challenges to the power system. Control of power system, as one of the fundamental requirements in the operating power system, considers reliable production and delivery of power while maintaining system voltage and frequency within permissible boundaries.

Frequency is one of the most important factors in power quality and in order to maintain its stability, generation and demand should always be matched. In the interest of minimising frequency deviation in the power system, ancillary services are used [4]. Conventionally, there are manual and automatic operating frequency reserves – primary regulation (PR), secondary regulation (SR) and tertiary regulation (TR). By replacing conventional generators with RES, the system frequency is subjected to more frequent and larger deviations which, consequently, lead to the less secure and unstable power system. Accordingly, new balancing reserves have to be used and provided to the power system [5]. For that reason, the integration of energy storage systems (ESSs) to the system is suggested.

Schlegel *et al*. [6] have presented different ESS solutions based on storage capacity and discharged time as a support for the frequency regulation. In [7], the performance of the ESS with a limited capacity, which are providing PR, is discussed. As fast-acting ESSs when compared to conventional generators and with the capability to act as a controllable source and sink of electricity, battery ESSs (BESSs) are considered as a prominent solution for system services [6, 8]. BESS support in terms of PR in RES dominated power system is researched in [9] where the performance of BESS with limited capacity and different control strategies is investigated. Oudalov *et al*. [8] implemented a control algorithm with adjustable state of charge (SOC) limits for BESS. In terms of PR, one of the proposed algorithms is considered for optimal BESS operation.

The novelty of this work combines modelling of BESS including a suitable PR strategy with variable droop, which imitates governors' proportional control and their implementation in an interconnected two-area power system for which dynamic simulations are conducted in DIgSILENT PowerFactory.

The main objective of this work is to develop PR to integrate and test the performance of BESS in an interconnected two-area power system with variable power penetration from RES in order to explore the capability of providing frequency regulation to the power system with RES and BESS.

An overview of frequency stability theorem and theory behind PR is given in Section 2. Section 3 presents the models of different components. Grid model and simulation scenarios to be tested and analysed are discussed in Section 4. In Section 5, the results and discussion of tested scenarios are presented. Additionally, sensitivity analysis for sizing of BESS units is performed. Section 6 gives the conclusion of this work.

2 Frequency regulation in conventional power system

PRs are automatic reserves activated within seconds after the disturbance with complete deployment within 30 s. According to the European Network of Transmission System Operators for Electricity (ENTSO-E) [10, 11], the frequency range, before primary control is provided to the system, is within ±20 mHz and primary control must be supplied before frequency deviation exceeds ±200 mHz. SRs are activated after the frequency is maintained by PR. Meaning, within 30 s to 15 min after the disturbance with the purpose of restoring and maintaining frequency to its nominal value and replenish used PRs. TRs are provided manually with tertiary control, which is slower than the previous two mentioned. The purpose of TR is to absolve the activated SR in a time interval from minutes to hours [12, 13]. All three regulation processes are shown in Fig. 1.

2.1 Primary regulation

In a conventional power system, PR is provided by generators' governor. Generator speed is directly coupled to the grid frequency and consequently, active power as well. The relation between inertia response, as the change in frequency of the synchronous

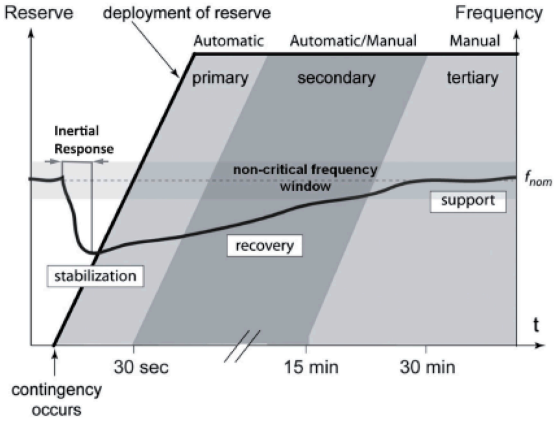

Fig. 1 *Frequency regulation processes [14]*

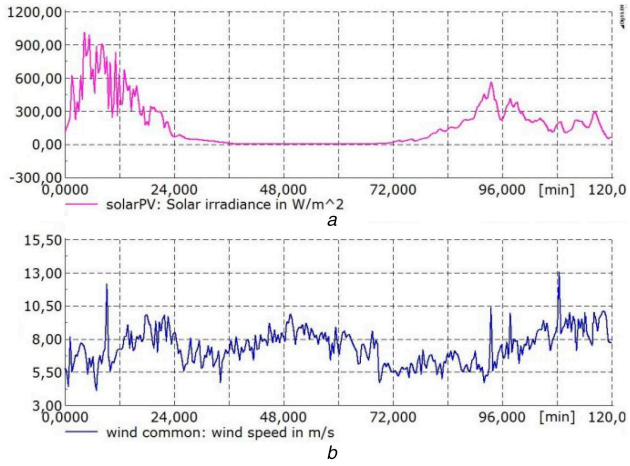

Fig. 2 *Data profiles*
(a) Solar irradiance data, ***(b)*** Wind speed data

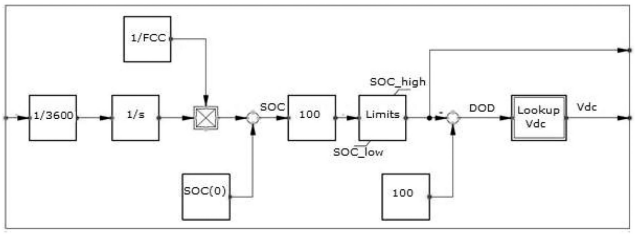

Fig. 3 *BESS model*

generator and power imbalance, is called swing equation and is expressed in [15] as follows:

$$\frac{2 \cdot H \cdot S_{\mathrm{B}}}{f_{\mathrm{m}}} \cdot \frac{\mathrm{d}f_{\mathrm{m}}}{\mathrm{d}t} = P_{\mathrm{m}} - P_{\mathrm{e}}, \tag{1}$$

where f_{m} denotes the rotating frequency of the machine, H inertia constant, S_{B} rated power of the generator, P_{m} mechanical power supplied by the generator and P_{e} is the electric power demand. H is the time at which machine is supplying rated power with kinetic energy stored.

In the case of loss of generation or sudden increase of the electrical load, system frequency drops from its nominal value. Generator governor has the purpose of bringing the frequency to its nominal value and that type of control is called droop control. Speed droop R is the ratio of frequency and power output change [16] and it is given in the following expression:

$$R = \frac{\Delta f}{\Delta P}, \tag{2}$$

where Δf denotes frequency change and ΔP power output change.

3 Dynamic models of the components

All dynamic models, including BESS and RES, the interconnected two-area system and PR strategies are developed and simulated using DIgSILENT simulation language (DSL) models in DIgSILENT PowerFactory software.

3.1 Renewable energy sources (RES) models

Solar photovoltaic (PV) output power of the module is calculated as follows:

$$P_{\mathrm{PV}} = S \cdot A \cdot \eta \cdot PR, \tag{3}$$

where P_{PV} is the output power of the PV module, S is the solar irradiance (W/m^2), A is the area of the PV module (m^2), η is the efficiency of the PV module and PR is the performance ratio.

The output power of the wind turbine (WT) is given by the following expression:

$$P_{\mathrm{WT}} = \frac{1}{2}\rho C_{\mathrm{p}} A v_{\mathrm{w}}^3, \tag{4}$$

where P_{WT} is the output power of WT (W), ρ is the air density (kg/m$_3$), C_{p} is the power coefficient, A is the WT swept area (m^2) and v_{w} is the wind speed at hub height (m/s). Given wind speed depends on the wind speed measured at the reference height and roughness of the terrain.

Based on the real data provided from the laboratory facility at Aalborg University, profiles of wind speed at the reference height and solar irradiance for 2 h are shown in Fig. 2.

3.2 BESS model

The SOC is the relevant parameter when it comes to the BESS control for PR support. As stated in [17], 'Coulomb counting' is the method used to calculate SOC of BESS. Based on [18], the mathematical expression of the given method is as follows:

$$\mathrm{SOC}(t) = \frac{1}{\mathrm{FCC}} \int i(\tau)\mathrm{d}\tau + \mathrm{SOC}(0), \tag{5}$$

where FCC is the full charged capacity or rated BESS capacity in Ah. SOC(0) is expressed as

$$\mathrm{SOC}(0) = \frac{C(0)}{\mathrm{FCC}}, \tag{6}$$

where $C(0)$ is the initial charge of the BESS. The BESS model based on (5) and (6) is shown in Fig. 3. The available data is given in the Appendix. It should be pointed out that even though the SOC value is obtained, in the look up table depth of discharge (DOD) is used due to the correlation of DOD and voltage. DOD is representing the percentage of BESS maximum capacity that has been discharged, while SOC is representing present BESS capacity as a percentage of BESS maximum capacity.

The main concept of BESS control is to imitate governor's droop characteristic such as in conventional generators. In [9], different control strategies, which consider the SOC change of BESS, are analysed. Based on the presented results, the strategy with variable speed droop and SOC limits for normal and an emergency operation is considered to be the most suitable one in the aspect of frequency regulation (FR). The value of speed droop is changeable and dependent on the SOC value. $\mathrm{SOC}_{\mathrm{high}}$ and $\mathrm{SOC}_{\mathrm{low}}$ are for normal operation and $\mathrm{SOC}_{\mathrm{max}}$ and $\mathrm{SOC}_{\mathrm{min}}$ are for emergency operation. The values of the limits are given in the Appendix

$$R = \begin{cases} R_{\max}\left[1 - ((\mathrm{SOC} - \mathrm{SOC}_{\mathrm{high}})/\mathrm{SOC}_{\min} - \mathrm{SOC}_{\mathrm{high}})^2\right], \Delta f \le 0 \\ R_{\max}\left[1 - ((\mathrm{SOC} - \mathrm{SOC}_{\mathrm{low}})/(\mathrm{SOC}_{\min} - \mathrm{SOC}_{\mathrm{low}}))^2\right], \Delta f > 0 \end{cases}, \tag{7}$$

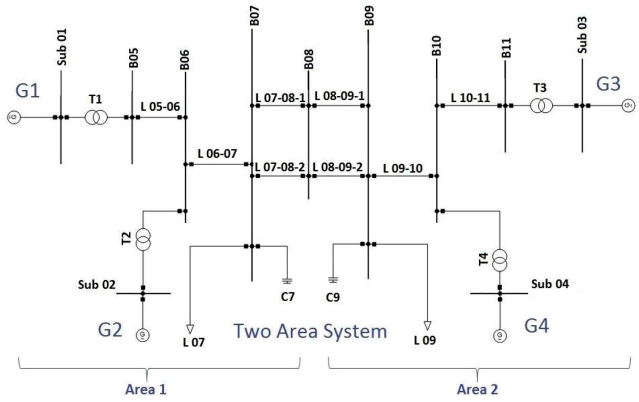

Fig. 4 *Two-area system model [16]*

Table 1 Simulated and calculated values of the relevant parameters

Load change event, %	1	5	15
*G*1 active power output, MW	702.24	713.68	748.88
*G*2 active power output, MW	703.12	716.32	757.68
*G*3 active power output, MW	712.8	724.24	759.44
*G*4 active power output, MW	702.24	713.68	748.00
Δf, Hz	−0.026	−0.057	−0.150
ΔP_{12}, MW	−4.84	−28.93	−100.69

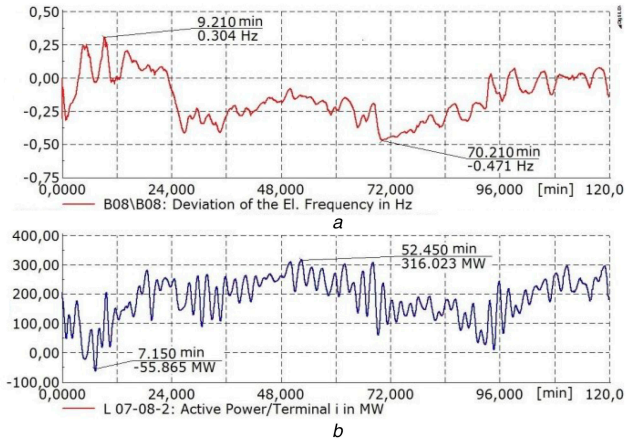

Fig. 5 *System with RES integration*
(a) Frequency deviation on the tie line, ***(b)*** Active power flow from area 1 to area 2

where $R_{\max}$ is the maximum value of the speed-droop expressed in Hz/W and Δf is the system frequency deviation in Hz.

Since the BESS provides PR for negative and positive frequency deviation, calculation of BESS speed droop will depend on both, the sign of the frequency deviation and SOC value.

4 Grid model and simulation scenarios

4.1 Model of the interconnected two-area power system

The model of the interconnected two-area system is based on [16] and shown in Fig. 4 and it is used as a test case network. Two areas are connected with a tie line consisting of two lines and each area has five buses.

The main aim to accomplish when it comes to the tie line power and frequency deviation is to keep frequency at its nominal value and have a scheduled tie line flow.

The frequency deviation in the case of disturbances in area 1 [16, 19] is calculated as follows:

$$\Delta f = \frac{-\Delta P_{\mathrm{L1}}}{(1/R_{\mathrm{eq1}}) + (1/R_{\mathrm{eq2}})}, \tag{8}$$

where ΔP_{L1} is the non-frequency sensitive load change and $1/R_{\mathrm{eq1}}$ and $1/R_{\mathrm{eq2}}$ are the sum of reciprocal values of speed-droops of each generator in area 1 and area 2, respectively.

4.2 Simulation scenarios

Simulations on frequency regulation for a given system are performed for three main cases. Firstly, a case with only conventional generators providing PR is analysed.

Meaning, testing of dynamic models of steam- and gas-based power plants, representing conventional generators, has been performed in order to study and understand their dynamics subjected to disturbances in the interconnected two area power system. Chosen gas and steam turbine models are gov_GAST and gov_IEEEG1, respectively, and are part of DIgSILENT PowerFactory global library. Secondly, RES components, such as WT and PV, are integrated into the system with only conventional generators. In area 1, generator (G) *G*2 is replaced by the wind farm while in area 2, a PV system is connected to the same bus as generator *G*4. Additionally, the active power output of *G*4 is reduced by 200 MW. As a final case, BESS is integrated into both areas of the system and connected to the same buses as RES. This has been done in order to evaluate and analyse its impact on system frequency deviation. The MW size of aggregated BESS units is evaluated based on sensitivity analysis conducted. It should be noted that RES components in an interconnected two-area system are represented through aggregated MW size models of WT and PV. Profiles with high fluctuations are chosen which means that for PV minimum and maximum output power are 0 and 880 MW, respectively. For WT minimum is 90 MW while the maximum is 880 MW. Average output powers for PV and WT for the observed period are 140 and 534 MW, respectively. The capacity of all units is given in the Appendix.

5 Results and discussion

5.1 Frequency regulation in a conventional system

Simulation results for frequency deviation and active power flow are shown in Table 1 for the case of different load increase events in area 1. It can be observed that with the higher load increase, frequency deviation on the tie line is higher and consequently power produced from the generators is higher to meet additional load in the system. Moreover, active power flow from area 1 to area 2 is lower as a result of higher power required by the load in area 1 and it deviates from the scheduled power flow of 408 MW. Lastly, it should be pointed out that the frequency reaches steady state after every simulated event and system is stable, due to the PR provided by conventional generators but its value is not within a dead band of ±20 mHz.

5.2 Frequency regulation with RES integration

Fig. 5*a* shows frequency deviation on the tie line while Fig. 5*b* shows active power flow from area 1 to area 2 on the tie line. As it can be observed, active power flow is variable and most of the time is positive due to the fact that active power is being exported from area 1 to area 2. Furthermore, frequency deviation is negative for most of the period, as a result of the decrease of RES generation. In such cases, conventional power generators need to increase their power production.

Maximum positive frequency deviation is 0.304 Hz. Maximum negative frequency deviation in area 1 and area 2 is −0.471 Hz. It should be pointed out that both values exceed dead band of ±20 mHz. In Fig. 5*b*, active power flow from area 1 to area 2 is shown only in one line and the peak value of active power transported to area 2 is 316.023 MW, while to area 1 is 55.865 MW in one line. Since the scheduled power is 204 MW in one line, 116 MW is the deviation from the scheduled value for that line.

As seen in Fig. 6, during periods of low WT generation, *G*1 is increasing its active power output to meet the load in area 1. Due to the reduced PV power production, *G*3 and *G*4 are increasing power generation. The output power of *G*3 is higher as its nominal output power was not previously reduced. Additionally, it may be

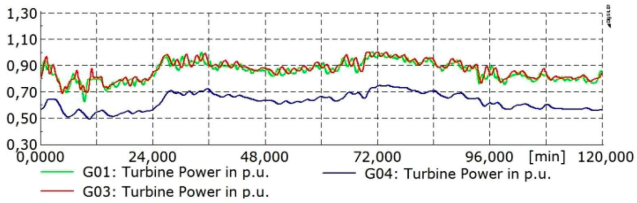

Fig. 6 *G1, G3, and G4 active power output in the system with RES integration*

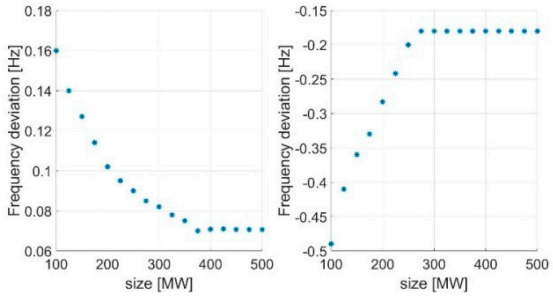

Fig. 7 *Sensitivity analysis results*

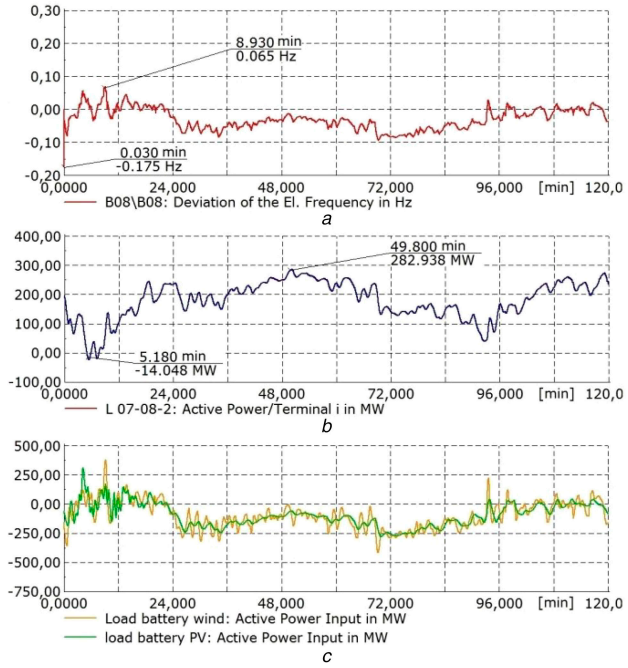

Fig. 8 *System with BESS integration*
(a) Frequency deviation on the tie line, ***(b)*** Active power flow from area 1 to area 2, ***(c)*** BESS active power input

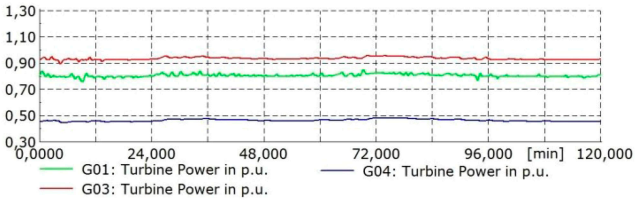

Fig. 9 *Generators active power output*

observed that *G*3 production around 72 min is at the peak since the RES power production is the lowest.

Based on the aforementioned observations, two main scenarios may be analysed. The first scenario is when the frequency deviation on the tie line is positive. Generally, frequency deviation is positive when there is power overproduction. In this case, WT output power is very high and thus, *G*1 is not producing that much and overall power production in area 1 is higher than the load. Also, PV power production is high and consequently power production from *G*3 and *G*4 is lower. As a result of high PV and WT power generation and lower amount of power produced by conventional generators, frequency deviation is very high due to the lack of PR reserves. The second case is when there is a low PV and WT power production in which *G*1, *G*3, and *G*4 are generating more power than RES. During this period, the power required by the load is higher than the power generation from PV, WT, and generators. Therefore, the frequency deviation is negative. Overall, frequency deviation is lower due to the higher amount of power produced by conventional generators as they can provide PR.

To conclude, frequency deviation is higher than in the case with only conventional generators. The main reason is the intermittent generation of RES. Therefore, as it is assumed, with the integration of RES, power system stability degrades. Thus, in order to improve power system frequency and, consequently, power system stability, BESSs are considered as a prominent solution. In the next subsection, it is investigated whether PR provided by BESS is sufficient enough to maintain frequency deviation within permissible limits.

5.3 Frequency regulation with BESS integration

To find a proper BESS size, sensitivity analysis is conducted in order to understand the impact of the relative BESS size on PR. It should be pointed out that the BESS size is considered to be aggregated in MW range representing the size of distributed BESS units.

The relevant factor considered for BESS sizing is frequency deviation. It is expected that frequency deviation decreases as the BESS size increases due to the higher amount of PR provided. Positive and negative frequency deviations are considered as BESSs need to store and supply power, respectively, with respect to the variability of RES. In Fig. 7, positive and negative frequency deviation of different BESS sizes in MW is shown. For positive frequency deviation, frequency saturates for sizes >375 MW, while for negative frequency, it occurs for a value of 275 MW. Hence, the chosen BESS size, based on the analysis conducted, is 400 MW.

As seen in Fig. 8*a*, frequency deviation is lower when the BESS is added to the system. Furthermore, it may be observed in Fig. 8*b* that the overall active power flow is less than in the case with RES integration. This is due to the BESS capability of storing energy in cases of overproduction and providing it in cases of underproduction as shown in Fig. 8*c*. Therefore, power flow from area 1 to area 2 is closer to the scheduled value of 204 MW in one line. Maximum and minimum frequency deviation values are 0.065 and −0.175 Hz, respectively, with a decrease of 0.239 and 0.296 Hz with respect to the previous case.

Conventional generators active power output is presented in Fig. 9. Generators output power is not fluctuating due to the fast BESS response. In addition, the active output power of *G*1 is more intermittent than the active power output of *G*3 and *G*4 as WT power production is subjected to higher and more frequent fluctuations than PV power production.

To conclude, with the integration of BESS in the grid, power system frequency stability is improved. Power flow from area 1 to area 2 is closer to the scheduled value of 204 MW in one line, and fluctuations in frequency are lower than in the case with the integration of RES.

5.4 Comparison of simulation results

In Table 2, results of frequency deviation are compared on the tie line for two cases, one with RES integration and another with additional support from the BESS.

To conclude, frequency deviation is the highest in the case with RES integration due to the lack of PR reserves. With the integration of the BESS to the grid, power system frequency stability is improved as frequency deviation is lower because of the PR provided by the BESS.

Furthermore, in all cases analysed, frequency steady state error is still present after PR is supplied to the system. In order to restore frequency to its nominal value, SR should be activated. Therefore, in a case of further analysis of power system frequency regulation, it is expected that with SR, frequency steady state error is

Table 2 Comparison of frequency deviations on the tie line for cases with RES integration and BESS integration

	Max Δf, Hz	Min Δf, Hz	Mean Δf, Hz	Standard deviation Δf, Hz
with RES	0.304	−0.471	−0.1514	0.1695
with BESS	0.065	−0.175	−0.0297	0.0307

eliminated and active power flow on the tie line is restored to the scheduled. As future work, the investigation of possible PR control from PV and WT units could be conducted. Moreover, the dynamic behaviour of the time variable load with considered load damping constant should be included. Furthermore, a more complex model of the BESS including its degradation behaviour could be studied. Finally, other types of ESSs or flexible loads could be examined in order to provide frequency regulation. In addition to suggested improvements, the study can be continued with the integration of SR including participation factors, ramping of various units participating in frequency regulation and system performance during contingencies.

6 Conclusion

This study has presented the integration of the BESS in RES dominated power system in order to show its impact on power system frequency stability. As expected, due to the intermittent nature of RES, the power system is being subjected to fluctuations in frequency and, consequently, frequency deviations are higher and more frequent. Based on the obtained results, in the system with a high installed capacity of RES, support in terms of frequency regulation from conventional generators, is still required. While the results for the system with an integrated BESS show that the power system frequency is more stable and subject to a smaller number of fluctuations.

7 References

[1] Danish Energy Agency: 'The Danish energy model'. 2016, Available at https://ens.dk/sites/ens.dk/files/contents/material/file/the_danish_energy_model.pdf, accessed 6 October 2017

[2] Energinet.dk: 'New record-breaking year for Danish wind power'. 2016 January. Available at https://en.energinet.dk/About-our-news/News/2017/04/25/New-record-breaking-year-for-Danish-wind-power, accessed 15 September 2017

[3] Danish Energy Agency: 'Energy in Denmark – a green transition'. 2016. Available at https://www.comillas.edu/images/catedraBP/Foro_2016/Larsen_Energy%20in%20Denmark_a%20green%20transition-Energistyrelsen%202016.pdf, accessed 01 October 2017

[4] EURELECTRIC: 'Ancillary services'. 2003. Available at http://www.eurelectric.org/Download/Download.aspx?DocumentFileID=25426, accessed 6 October 2017

[5] Aho, J., Buckspan, A., Laks, J., *et al.*: 'A tutorial of wind turbine control for supporting grid frequency through active power control'. American Control Conf. (ACC), Montreal, Canada, 2012, pp. 3120–3131

[6] Schlegel, S., Schwerdfeger, R., Westermann, D.: 'Involvement of flexible loads in transmission system operation'. Third IEEE PES Innovative Smart Grid Technologies Europe (ISGT Europe), Berlin, Germany, 2012, pp. 1–5

[7] Wandelt, F., Gamrad, D., Deis, W., *et al.*: 'Comparison of flywheels and batteries in combination with industrial plants for the provision of primary control reserve'. IEEE PowerTech, Eindhoven, 2015, pp. 1–6

[8] Oudalov, A., Chartouni, D., Ohler, C.: 'Optimizing a battery energy storage system for primary frequency control', *IEEE Trans. Power Syst.*, 2007, **22**, (3), pp. 1259–1266

[9] Li, X., Huang, Y., Huang, J., *et al.*: 'Modeling and control strategy of battery energy storage system for primary frequency regulation'. Int. Conf. on Power System Technology, Chengdu, China, 2014

[10] ENTSO-E: 'Frequency stability evaluation – criteria for the synchronous zone – requirements'. March 2016. Available at https://www.entsoe.eu/Documents/SOC%20documents/RGCE_SPD_frequency_stability_criteri, accessed 6. 10. 2017

[11] Energinet.dk: 'Ancillary services to be delivered in Denmark'. September 2017. Available at https://en.energinet.dk/Electricity/Rules-and-Regulations, accessed 6. 10. 2017

[12] Das, K., Litong-Palima, M., Maule, P., *et al.*: 'Adequacy of operating reserves for power systems in future European wind power scenarios'. IEEE Power & Energy Society General Meeting, Denver, CO, USA, 2015, pp. 1–5

[13] Das, K., Altin, M., Hansen, A.D., *et al.*: 'Primary reserve studies for high wind power penetrated systems'. IEEE PowerTech, Eindhoven, Netherlands, 2015, pp. 1–6

[14] Knap, V., Chaudhary, S.K., Stroe, D.-I., *et al.*: 'Sizing of an energy storage system for grid inertial response and primary frequency reserve', *IEEE Trans. Power Syst.*, 2016, **31**, (5), pp. 3447–3456

[15] Ulbig, A., Borsche, T.S., Andersson, G.: 'Impact of low rotational inertia on power system stability and operation'. IFAC World Congress 2014, Cape Town, South Africa, 2014

[16] Kundur, P.: '*Power systems stability and control*' (McGraw-Hill, New York, NY, USA, 1994)

[17] Pilai, J., Bak-Jensen, B.: 'Integration of vehicle-to-grid in the western Danish power system', *IEEE Trans. Sustain. Energy*, 2011, **2**, (1), pp. 12–19

[18] Oya, M., Takaba, K., Lin, L., *et al.*: 'Accurate SoC estimation of lithium-ion batteries based on parameter-dependent state-space model'. 2015 15th Int. Symp. on Communications and Information Technologies (ISCIT), IEEE Conf. Publications, Nara, Japan, 2105, pp. 37–40

[19] Saadat, H.: '*Power system analysis*' (PSA publishing, Atlanta, GA, USA, 2014, 3rd edn.)

8 Appendix

$G1 = 700$ MW, $G2 = 700$ MW, $G3 = 719$ MW, $G4 = 700$ MW, $1/R1 = 1/R3 = 4.7\%$, $1/R2 = 1/R4 = 4\%$, $L07 = 967$ MW, $L09 = 1767$ MW, $P_{WT} = 880$ MW, $P_{PV} = 880$ MW, $P_{BESS} = 400$ MW.

BESS data: FCC = 60 Ah, $SOC(0) = 0.5$, $SOC_{min} = 0.1$, $SOC_{max} = 0.9$, $SOC_{high} = 0.8$, $SOC_{low} = 0.2$.